Japanese Journal of Applied Physics
Vol. 47, No. 1, 2008, pp. 689–693

Imaging Characteristics and Quantum Efficiency: Key Properties for Pixelless Far-Infrared Semiconductor Upconversion Imaging Devices

Leke WU and Wenzhong SHEN*

Laboratory of Condensed Matter Spectroscopy and Opto-Electronic Physics, Department of Physics, Shanghai Jiao Tong University, 1954 Hua Shan Road, Shanghai 200030, P. R. China

(Received July 12, 2007; accepted October 31, 2007; published online January 22, 2008)

Employing the concept of photon frequency upconversion, we have proposed two types of semiconductor upconverters to realize pixelless far-infrared (FIR) imaging. The upconverter consists of a GaAs FIR homojunction interfacial work-function internal photoemission detector integrated with a GaAs/AlGaAs near-infrared light-emitting diode (LED), or GaN/AlGaN mid-IR/FIR dual-band heterojunction detector with a GaN/AlGaN violet LED. We have studied in detail the dependences of the modulation transfer function and quantum efficiency of the upconverters on various device parameters. Through the application of resonant cavity to the GaAs-based upconverter, we can expect sharp and high-resolution image and improved quantum efficiency. In addition, due to the large light absorption in the GaN/AlGaN heterojunction detector, the quantum efficiency of the GaN-based upconverter is much higher than that of GaAs-based one. [DOI: 10.1143/JJAP.47.689]

KEYWORDS: imaging, quantum efficiency, far-infrared, upconversion, pixelless

1. Introduction

Silicon charged coupled devices (Si CCDs) are high performance and low cost image sensors with the detection wavelength up to ~1 μm. Currently, the mid-infrared (MIR) imaging is achieved by expensive InSb and HgCdTe arrays, while there are no image sensors commercially available for the far-IR (FIR) radiation. The photon frequency upconversion concept[1] provides possibilities for semiconductor detection imaging of arbitrary wavelength light. By integrating an IR photodetector with a near-IR (NIR) light-emitting diode (LED) under a forward bias, one can expect the increase of the potential drop across the LED due to the reduction of the detector resistance upon IR radiation. The upconverted image of the IR object is realized by the short NIR emission from the LED, which falls into the efficient imaging range of the Si CCD. With sufficient number of periodic structures in detectors, the nonuniformity of the incoming IR light can be almost maintained in the photocurrent, and therefore this kind of imaging device is not necessarily separated into pixels. Liu *et al.*[2] have demonstrated successfully the pixelless MIR detection imaging with an upconverter consisting of a GaAs/AlGaAs quantum well infrared photodetector and an InGaAs/GaAs LED.

In this paper, we propose two types of pixelless FIR semiconductor upconversion imaging devices. One is the integrated structure of a GaAs FIR homojunction interfacial work-function internal photoemission (HIWIP) detector[3] with a GaAs/AlGaAs NIR LED, the other is a GaN/AlGaN MIR/FIR dual-band heterojunction detector[4] with a GaN/AlGaN violet LED. Since the key properties to practical application of the FIR upconverters are good image quality and high quantum efficiency, we have examined in detail the effects of device parameters on the modulation transfer function (MTF) and quantum efficiency of the upconverters. With a resonant cavity, the GaAs-based upconverter has good image quality and improved quantum efficiency. As a result of large light absorption in the GaN/AlGaN heterojunction detector, the GaN-based upconverter has much higher quantum efficiency than that of the GaAs-based one.

*E-mail address: wzshen@sjtu.edu.cn

2. Theoretical Method

The schematic view of the integrated structure for the GaAs-based FIR HIWIP detector (N periods of emitter/intrinsic layers) and NIR LED is shown in Fig. 1(a). Under a certain bias and upon nonuniform FIR radiation, the carriers in the emitter layers of the FIR detector are photoexcited into the high energy states, and diffuse to the emitting interfaces with the transport probability determined by the diffusion length. Those photocarriers reaching the interfaces tunnel through the interfacial barriers resulting from the band gap narrowing effect, and then collected by the image force at the interfaces.[3] The nonuniform photocurrent from the FIR HIWIP detector injects into the active region of NIR LED, most of the photocarriers recombine there due to the confinement of wide-gap clad layers, leading to the emission of NIR light through the radiative recombination. The output NIR light can be directly detected by Si CCD, therefore, the upconversion imaging from FIR to NIR could be realized.

Taking the p-GaAs FIR HIWIP detector as an example, according to the detection mechanism, the ratio G of photocarriers across the interfacial barriers between the emitter and intrinsic layers has the form:[5]

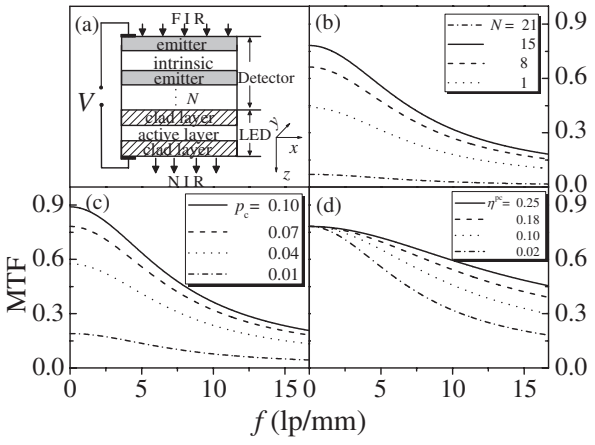

Fig. 1. (a) Schematic view of the cross section of a FIR upconverter by integrating a detector with an LED. The dependences of MTF on spatial frequency f under various (b) number of emitter layers N at $p_c = 0.07$ and $\eta^{pc} = 0.02$, (c) capture probability p_c at $N = 21$ and $\eta^{pc} = 0.02$, and (d) extraction efficiency η^{pc} of LED at $N = 21$ and $p_c = 0.07$.

$$G = [1 - \exp(-2\alpha_p w_e)] \exp\left(-\frac{w_e}{l}\right) \exp\left(-\frac{x_b}{l_s}\right) \quad (1)$$

where the coefficient of free carrier absorption is $\alpha_p = 8.28 \times 10^{-16}\,\mathrm{cm}^2 \times N_a$[3] with N_a the doping concentration of the p-GaAs emitter layers, w_e is the emitter layer thickness, l is the characteristic diffusion length, $x_b = \sqrt{q/16\pi\varepsilon E}$ is the distance from the interface to the barrier maximum in the GaAs FIR HIWIP detector with q the unit charge, ε the dielectric constant, and E the electric field, and $l_s = 276 \pm 2$ Å[3] is the hole scattering length in the image force well.

Employing the spectral decomposition approach, the radiation photon flux distribution of a two-dimensional sine target is assumed $\phi^{in} = \phi_0^{in} + \phi_f^{in} \cos 2\pi \boldsymbol{fr}$, with $\boldsymbol{r} = (x, y)$, ϕ_0^{in} the average photon flux of the incoming FIR radiation, f the spatial frequency, and ϕ_f^{in} the signal part amplitude of the sine wave. We neglect the impurity compensation in the p-GaAs emitter layers, the carrier diffusion along the axis z, and the carrier drift along axes x and y. Assuming that the in-plane potential is uniform within the emitter layers, we can write the current continuity equation of the carrier transport in the FIR HIWIP detector.[5] As a result, the output photocurrent density $j = j_0 + j_f \cos 2\pi \boldsymbol{fr}$ can be obtained, with the average photocurrent density j_0 of

$$j_0 = \frac{qG\phi_0^{in}}{p_c} \quad (2)$$

and the signal part amplitude of the output current density j_f of

$$j_f = qG\phi_f^{in} \exp(-4\pi^2 l^2 f^2) \frac{1 - (1 - p_c)^N \exp(-4\pi^2 l^2 f^2 N)}{1 - (1 - p_c)\exp(-4\pi^2 l^2 f^2)} \quad (3)$$

with N the number of emitter layers and p_c the capture probability of photocarriers.[6]

Following the analysis for NIR LED in ref. 7, starting from the carrier diffusion equation in the LED active region and considering the photon recycling effect,[8] we can get the average photon flux ϕ_0^{out} and the signal part amplitude ϕ_f^{out}:

$$\phi_0^{out} = \frac{\eta^{pc}\eta_{int} j_0}{q\left[1 - (1 - \eta^{pc})\left(\frac{\alpha_1}{\alpha_2}\right)\eta_{int}\right]} \quad (4)$$

$$\phi_f^{out} = \frac{\eta^{pc}\eta_{int} j_f}{q\left[1 + 4\pi^2 f^2 l_d^2 - (1 - \eta^{pc})\left(\frac{\alpha_1\alpha_2}{\alpha_2^2 + 4\pi^2 f^2}\right)\eta_{int}\right]} \quad (5)$$

here η^{pc} is the extraction efficiency of NIR photons in LED, η_{int} is the internal quantum efficiency of the LED, l_d is the diffusion length of carriers in the GaAs active layer. $\alpha_1 = \alpha_a\Gamma$, $\alpha_2 = \alpha_a\Gamma + \alpha_c(1 - \Gamma)$, where α_a and α_c are the photon absorption coefficients for the active region and surrounding layers, respectively, and $\Gamma = d_a/(d_a + d_c)$ with d_a the thickness of the LED active layer and d_c the net thickness of other layers between the reflecting surfaces.

3. Results and Discussion

3.1 Imaging characteristics of GaAs-based upconverter

To investigate the imaging characteristics of the GaAs-based upconverter, we study the MTF, which is ratio of the image contrast ($\phi_f^{out}/\phi_0^{out}$) to the object contrast (ϕ_f^{in}/ϕ_0^{in}) at different spatial frequency f. From eqs. (2)–(5), the MTF can be easily obtained. We have optimized in Fig. 1 the main parameters of the FIR HIWIP detector and NIR LED influencing MTF. Note that except for the examined one, the calculations have been done under the optimal parameters throughout the paper. In Fig. 1(b), it is clear that the MTF increases with N. In addition, the spatial distribution of incoming FIR radiation intensity could be well maintained in the photocurrent density of the FIR HIWIP detector with large N, the HIWIP detector based FIR upconverter is therefore not necessarily separated into pixels.[9] However, N can not be increased arbitrarily due to the impact ionization process in the FIR HIWIP detector. The relationship between N and the device parameters is given by $2^{N-2}q^2D \le \varepsilon_0\Delta A$,[3] with D the thickness of barrier layer, ε_0 the dielectric constant of vacuum, Δ the ionization barrier, and A the optical window area. Theoretical estimation with these parameters yields $N \le 21$ as a limit. Figure 1(c) shows that the image quality is improved with the increase of capture probability p_c, it is understandable since the nonuniform photocurrent will decrease at a slower rate than the uniform one with p_c, as can be seen from eqs. (2) and (3). Thus, the large p_c leads to the enhancement of the image contrast and increase of the MTF.

In the normal LED, the small critical cone angle imposed by Snell's law covers a solid angle of only $\approx (1/4n^2) \times 4\pi$ steradians, resulting in a low extraction efficiency η^{pc} of photons.[7] In case of GaAs/AlGaAs NIR LED, the extraction efficiency is only ~2%. Applying a resonant cavity constructed by the distributed Bragg reflectors (DBRs) to the LED, the preferential propagation direction of the NIR photons can be forced from total reflection regime toward the extraction cone, leading to a large η^{pc}. We have predicted through transverse electric–transverse magnetic (TE–TM) decomposition method[10] that with the appropriate resonant cavity design, η^{pc} can be achieved as high as 25%.[7]

Figure 1(d) displays the relationship between the MTF and η^{pc} of NIR photons in LED. In case of small η^{pc}, the NIR photon needs more reincarnation cycles to escape the LED in the photon recycling process,[8] so the diffusion of the photocarriers in the LED is significant, which can induce the imaging smearing. Within a resonant cavity, η^{pc} is high, as a result of few reincarnation cycles needed by a NIR photon to escape, the diffusion of NIR photon is negligible, which leads to the improved image quality.

It should be noted that due to the application of DBR resonant cavity, the NIR photons leaked from the LED can be effectively blocked from entering the FIR HIWIP detector,[7] thus the crosstalk induced by the leaked NIR photons reabsorbed in the emitter layers of FIR HIWIP detector can be avoided. We also note that in the FIR upconverter with the resonant cavity, MTF(f)/MTF(0) is always larger than 0.5 in the whole spatial frequency range, indicating that the image with perceived sharpness and resolution could be expected even in size of details.

3.2 Quantum efficiency of GaAs-based upconverter

The other important property for the upconverter is the quantum efficiency $\eta(f) = \phi_f^{out}/\phi_f^{in}$, which can be yielded from eqs. (3) and (5). We start with the dependence of

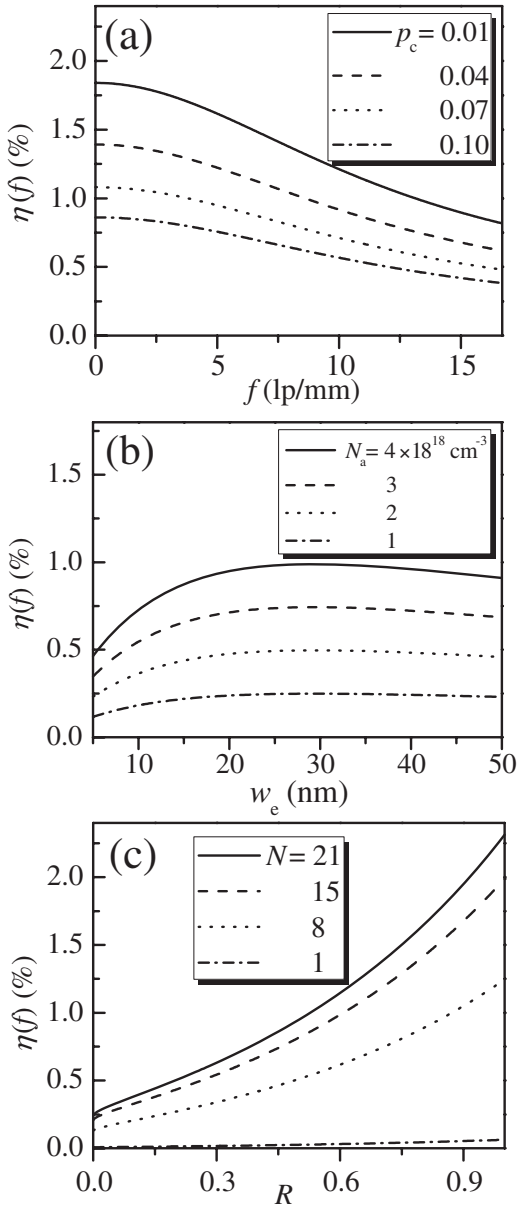

Fig. 2. Quantum efficiency $\eta(f)$ of the FIR upconverter as functions of (a) spatial frequency f and capture probability p_c under $N_a = 4 \times 10^{18}\,\mathrm{cm}^{-3}$, $w_e = 20\,\mathrm{nm}$, $N = 21$, and $R = 0.9$, (b) thickness w_e and doping concentration N_a of emitter layers under $p_c = 0.07$, $f = 5\,\mathrm{lp/mm}$, $N = 21$, and $R = 0.9$, and (c) reflectivity R of the bottom mirror and number of emitter layers N under $p_c = 0.07$, $f = 5\,\mathrm{lp/mm}$, $N_a = 4 \times 10^{18}\,\mathrm{cm}^{-3}$ and $w_e = 20\,\mathrm{nm}$.

$\eta(f)$ on the device parameters of FIR HIWIP detector. Figure 2(a) shows $\eta(f)$ at different capture probability p_c. We can see that the FIR radiation can be upconverted with different efficiencies at different f, and $\eta(f)$ is high for the large scale of image (small f), while low for the small size of image (large f). At high p_c, more carriers will be captured during the transport, the photocurrent driving the LED is reduced, leading to a small $\eta(f)$. In the following analysis, in view of convenience, we study the relationship between $\eta(f)$ and other parameters at a characteristic spatial frequency of 5 lp/mm.

Figure 2(b) presents the dependences of $\eta(f)$ on the doping concentration N_a and emitter layer thickness w_e. It is found that $\eta(f)$ increases with w_e first, and then tends to

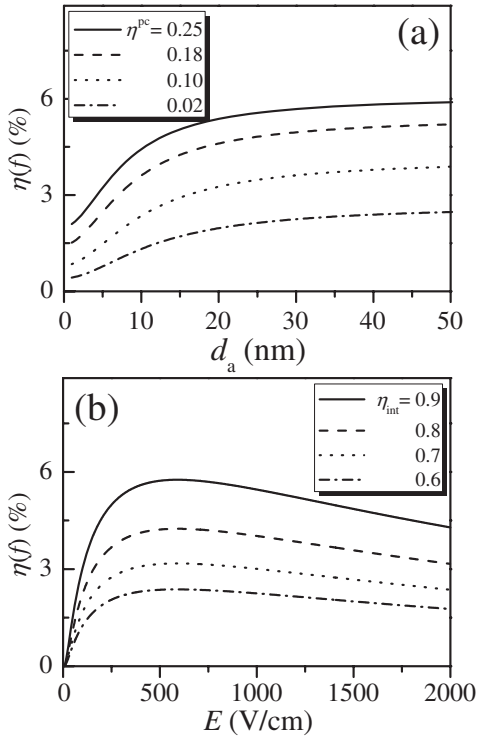

Fig. 3. Dependences of quantum efficiency $\eta(f)$ of the FIR upconverter on (a) active layer thickness d_a and extraction efficiency η^{pc} of LED at $f = 5\,\mathrm{lp/mm}$, $\eta_{int} = 0.9$, and $E = 300\,\mathrm{V/cm}$, (b) internal quantum efficiency η_{int} of LED and electric field E under $f = 5\,\mathrm{lp/mm}$, $\eta^{pc} = 0.25$, and $d_a = 30\,\mathrm{nm}$.

saturation. When w_e is larger than the diffusion length of carriers (20–30 nm in p-GaAs[3]), only a fraction of carriers contributes to the output current density, while others will lose in the diffusion due to the scattering processes, and $\eta(f)$ saturates at $w_e \approx 20\,\mathrm{nm}$. At the same time, the FIR radiation is absorbed more sufficiently in the emitter layers with increasing N_a, resulting in the increase of the number of output NIR photons. Therefore, $\eta(f)$ increases with N_a. While N_a cannot be increased indefinitely, it is restricted by the Mott transition concentration ($\sim 5.02 \times 10^{18}\,\mathrm{cm}^{-3}$ in p-GaAs[11]), under which semiconductor changes into metal. So the appropriate doping concentration in the emitter layers should be $4 \times 10^{18}\,\mathrm{cm}^{-3}$.

We note that $\eta(f)$ of the FIR upconverter is only $\sim$1% with the present structure, not satisfying for the practical applications. To further optimize the FIR upconverter, we apply a bottom mirror consisting of a single period of undoped/doped GaAs layers to the FIR HIWIP detector, where the free carrier absorption will be enhanced in the emitter layers.[7] Under the resonant condition, G takes the form as in ref. 7. We have calculated the effects of N and reflectivity R of bottom mirror on $\eta(f)$, as demonstrated in Fig. 2(c). With larger R, more FIR radiation is reflected back by the bottom mirror and the absorption in the emitter layers is enhanced, resulting in higher $\eta(f)$. In case of the FIR HIWIP detector with $N = 21$, $\eta(f)$ can be achieved $\sim$2% after adding a 90% reflectivity of bottom mirror.

We focus further on the dependences of $\eta(f)$ on the parameters of LED and electric field E. Figure 3(a) shows the relationship between $\eta(f)$ and active layer thickness d_a at various η^{pc}. It is found that $\eta(f)$ increases and saturates with

d_a due to the increasing nonradiative recombination of the injected photocarriers in the active layer with large d_a.[12] In case of the LED with a DBR resonant cavity, as a result of few reincarnation cycles needed by an average NIR photons to escape, the optical parasitic optical losses and non-radiative recombination losses are less during the photon recycling process,[8] thus $\eta(f)$ increases with η^{pc}. At $\eta^{pc} = 25\%$, $\eta(f)$ can be boosted to 5–6%, significantly higher than that of normal GaAs-based FIR upconverter. Therefore, the employment of DBR resonant cavity can not only improve the image quality, but also enhance the quantum efficiency of the upconverter.

From Fig. 3(b), it is seen that $\eta(f)$ increases with the LED internal quantum efficiency η_{int}. At high η_{int}, the bimolecular radiative recombination will dominate the recombination process, and the photon recycling effect is intensified, so $\eta(f)$ increases. Simultaneously, $\eta(f)$ exhibits a maximum with the increase of E. Due to the possible impact ionization breakdown of neutral impurity atoms occurring in the intrinsic layers of the FIR HIWIP detector,[11] $\eta(f)$ increases steeply with E first, and then reaches the maximum. Further increase of E will induce the rapidly increase of dark current, resulting in the decrease of the FIR HIWIP detector responsivity and reduction of $\eta(f)$. According to the present quantum efficiency, in the practical upconversion experiments, the input FIR power density should be in the order of $\sim$mW/cm^2 to get the output NIR light detected by normal Si CCDs.

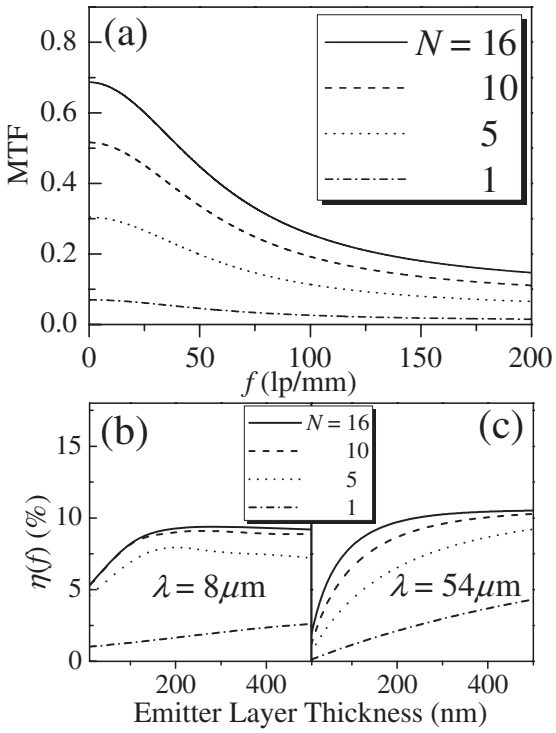

Fig. 4. (a) MTF of the dual-band upconverter as a function of spatial frequency f at different number of emitter layers N under $\eta^{pc} = 0.05$. The quantum efficiency $\eta(f)$ at $f = 5$ lp/mm of the dual-band upconverter as functions of emitter layer thickness and N under (b) $\lambda = 8\,\mu$m, and (c) $\lambda = 54\,\mu$m.

3.3 *GaN-based MIR/FIR dual-band upconverter*

The recently demonstrated GaN/AlGaN MIR/FIR dual-band heterojunction detectors[4] can foresee the dual-band pixelless imaging technology. On sapphire substrate, the main structure of single-period GaN/AlGaN heterojunction detector includes Si-doped n$^+$-GaN emitter (5×10^{18} cm^{-3}, 200 nm) and intrinsic $Al_xGa_{1-x}N$ barrier ($x = 0.026$, 600 nm) layers.[4] Based on the single period GaN/AlGaN heterojunction detector, we have investigated the integration of multi-period GaN/AlGaN heterojunction detector with a GaN/AlGaN violet LED to implement the dual-band pixelless upconversion imaging.

Figure 4(a) presents the spatial frequency dependence of MTF at different number of GaN emitter layers N in GaN/AlGaN heterojunction detector, the MTF increases with N at any f. In Si-doped GaN emitter layers, the ionization barrier is $\sim$31 meV, N is limited by the impact ionization process in the range $N \leq 16$. Due to the diffraction restriction, only image with $f \leq 1/\lambda$ could be resolved,[9] the object of MIR radiation will have much finer image than that of the FIR one, i.e., we can distinguish the MIR and FIR images though both components would be upconverted to the violet photons. Figures 4(b) and 4(c) give $\eta(f)$ as a function of emitter layer thickness at the typical MIR ($\lambda = 8\,\mu$m) and FIR ($\lambda = 54\,\mu$m) wavelengths, respectively. For the GaN/AlGaN with $N = 1$, due to the insufficient light absorption in the emitter layer, $\eta(f)$ increases with the emitter layer thickness. In case of multi-period one, the enough number of emitter layers can already guarantee the sufficient light absorption, and thicker emitter layers are not necessary. When the emitter layer thickness is over the carrier diffusion length in GaN ($\sim$250 nm), the quantum efficiency tends to saturation. Due to the long carrier diffusion length in GaN, the thickness of GaN emitter layers can be much larger than that of GaAs ones. Moreover, the absorption coefficient in GaN is higher than that in GaAs.[4] As a result, the quantum efficiency of the GaN-based upconverter can reach about 10%, even much higher than that of GaAs-based upconverter with resonant cavities.

4. Conclusions

Two types of FIR pixelless semiconductor upconversion imaging devices have been proposed, through the employment of photon frequency upconversion concept. One consists of a GaAs FIR HIWIP detector integrated with a GaAs/AlGaAs NIR LED, the other includes a GaN/AlGaN MIR/FIR dual-band heterojunction detector with a GaN/AlGaN violet LED. Satisfying image can be expected through the analysis of MTF, and the dependences of quantum efficiency on various device parameters have been investigated. Applying a resonant cavity to the GaAs-based upconverter, the quantum efficiency of the upconverter has been largely enhanced. As a result of fewer reincarnation cycles needed by an average NIR photon to escape in the photon recycling process, the existence of resonant cavity significantly improves the image quality. We have further shown that the quantum efficiency of the GaN-based upconverter is much higher than that of GaAs-based one.

Acknowledgments

This work was supported by the Natural Science Foundation of China under contract No. 60576067, Shanghai

Municipal Commission of Science and Technology Project of 05QMH1411, and the National Minister of Education Program for Changjiang Scholars and Innovative Research Team in University (PCSIRT).

1) P. W. Kruse, F. C. Pribble, and R. G. Schulze: J. Appl. Phys. **38** (1967) 1718.
2) H. C. Liu, J. Li, Z. R. Wasilewski, and M. Buchanan: Electron. Lett. **31** (1995) 832.
3) W. Z. Shen, A. G. U. Perera, H. C. Liu, M. Buchanan, and W. J. Schaff: Appl. Phys. Lett. **71** (1997) 2677.
4) G. Ariyawansa, M. B. M. Rinzan, M. Strassburg, N. Dietz, A. G. U. Perera, S. G. Matsik, A. Asghar, I. T. Ferguson, H. Luo, and H. C. Liu: Appl. Phys. Lett. **89** (2006) 141122.
5) L. K. Wu and W. Z. Shen: J. Appl. Phys. **100** (2006) 044508.
6) H. C. Liu: Appl. Phys. Lett. **60** (1992) 1507.
7) L. K. Wu and W. Z. Shen: IEEE J. Quantum Electron. **43** (2007) 411.
8) I. Schnitzer, E. Yablonovitch, C. Caneau, and T. J. Gmitter: Appl. Phys. Lett. **62** (1993) 131.
9) V. Ryzhii, H. C. Liu, I. Khmyrova, and M. Ryzhii: IEEE J. Quantum Electron. **33** (1997) 1527.
10) D. Delbeke, R. Bockstaele, P. Bienstman, R. Baets, and H. Benisty: IEEE J. Sel. Top. Quantum Electron. **8** (2002) 189.
11) A. G. U. Perera, H. X. Yuan, and M. H. Francombe: J. Appl. Phys. **77** (1995) 915.
12) N. F. Gardner, H. C. Chui, E. I. Chen, M. R. Krames, J.-W. Huang, F. A. Kish, S. A. Stockman, C. P. Kocot, T. S. Tan, and N. Moll: Appl. Phys. Lett. **74** (1999) 2230.